ELSEVIER

Chemical Engineering Journal 137 (2008) 294–301

Chemical Engineering Journal

www.elsevier.com/locate/cej

Synthesis of some bifunctional catalysts and determination of kinetic parameters for direct conversion of syngas to dimethyl ether

Ali Hadipour, Morteza Sohrabi *

Department of Chemical Engineering, Amirkabir University of Technology, Tehran 159145, Iran

Received 2 October 2006; received in revised form 22 April 2007; accepted 24 April 2007

Abstract

In the present study the catalyst preparation and modeling of the reaction kinetic for syngas transformation into dimethyl ether, using a mixture of a metallic oxides (CuO, ZnO and Al_2O_3) and an acidic component (γ-Al_2O_3) as the reaction catalyst, have been presented. Twenty-three catalysts samples were prepared according to a pre-designed research program consisting of four phases. In each phase, applying the experimental design method, a number of catalysts were synthesized by the co-precipitation method, using various amounts of metal nitrates. It was noted that the ZnO content of the catalyst, the nature of the precipitant agent, mass ratio of γ-alumina to total metal oxides and calcination temperature, had the highest impacts on the activity of the catalysts. Catalysts activity and kinetic measurements were carried out using a catalytic fixed bed microreactor. The operating temperature range was 230–300 °C and the pressure was 8 bar g. The experimental runs were performed applying a wide range of catalyst mass to molar feed ratios. A kinetic expression based on methanol synthesis and dehydration of the latter was devised and correlated with the experimental results. The degree of agreement between the two sets of data was higher than 85%.

Keywords: Dimethyl ether; Bifunctional catalysts; Activity measurement; Kinetic parameters

1. Introduction

Dimethyl ether (DME) is an intermediate in the preparation of a number of industrial chemicals. It has also found an increasing application in aerosol industry as an ozone friendly propellant. In addition, DME is used as an ultra-clean fuel for diesel engines [1–3].

Commercial production of dimethyl ether is achieved using either of the following two methods: (1) a two-step procedure consisting of methanol formation from synthesis gas followed by the dehydration of the latter and (2) a single step process, that is the direct formation of DME from synthesis gas. In comparison with the two-step method, the single-step procedure is attracting more attention for its dramatic economic value and theoretical significance [4].

A bifunctional catalyst for conversion of synthesis gas to DME normally contains two types of active sites used for methanol formation and methanol dehydration, respectively. These catalysts usually contain zinc, copper and aluminum oxides (for methanol formation) and γ-alumina (for methanol dehydration) and are prepared by the co-precipitation method [5].DME can be obtained directly from synthesis gas according to the following reactions:

- Methanol synthesis:

$$CO + 2H_2 \Leftrightarrow CH_3OH \tag{I}$$

- Methanol synthesis:

$$CO_2 + 3H_2 \Leftrightarrow CH_3OH + H_2O \tag{II}$$

- Water gas shift reaction:

$$CO + H_2O \Leftrightarrow CO_2 + H_2 \tag{III}$$

- Dehydration of methanol to DME:

$$2CH_3OH \Leftrightarrow CH_3OCH_3 + H_2O \tag{IV}$$

- Direct synthesis of DME:

$$2CO + 4H_2 \Leftrightarrow CH_3OCH_3 + H_2O \tag{V}$$

In the present study, based on Taguchi method [6], synthesis and activity measurement of some DME catalysts were per-

---

* Corresponding author. Fax: +98 21 66405847.
E-mail address: sohrabi@aut.ac.ir (M. Sohrabi).

1385-8947/$ – see front matter © 2007 Elsevier B.V. All rights reserved.
doi:10.1016/j.cej.2007.04.039

Nomenclature

E	activation energy
F	molar flow rate (mol/min)
H	heat of adsorption
KP1	equilibrium constant
KP2	thermodynamic equilibrium constant
K_1	kinetic parameter
K_2	adsorption constant of CO
K_3	adsorption constant of CO_2
K_4	adsorption constant of H_2O (Eq. (3))
K_5	kinetic parameter
K_6	adsorption constant of CH_3OH
K_7	adsorption constant of H_2O (Eq. (4))
P	pressure (bar g)
r	reaction rate (mol/min g cat.)
R	constant of gases (J/mol K)
T	temperature (K)
W	catalyst mass (g)
x	conversion
X	denotes concentration of copper oxide
y	mol fraction
Y	denotes concentration of zinc oxide
Z	denotes concentration of aluminum oxide

Greek letter

ϕ_v	volumetric flow (m^3/min)

formed within a program consisted of four phases. This method is a systematic application of design and analysis of experiments for the purpose of designing and improving product quality. In the recent years, the Taguchi method has become a powerful tool for improving productivity during research and development so that high quality products can be produced quickly and at low cost. Optimization of process parameters is the key step in Taguchi method in achieving a high quality without increasing the cost. This is because the optimization of process parameters can improve process performance characteristics and according to the Taguchi method these parameters are insensitive to variation of environmental conditions and other noise factors. Basically, classical process parameter design is complex and not easy to use, especially as large number of experiments have to be carried out when the number of the process parameter increases. To solve this task, the Taguchi method uses a special design of orthogonal arrays to study the entire process parameter space with a small number of experiments only. A loss function is then defined to calculate the deviation between the experimental value and the desired value. Taguchi recommends the use of the loss function to measure the performance characteristic deviation from the desired value. The value of the loss function is further transformed into a signal-to-noise (S/N) ratio. Usually, there are three categories of performance characteristic in the analysis of the S/N ratio, i.e. the lower-the-better, the higher-the-better and the nominal-the-better. The S/N ratio for each level of catalyst preparation parameters is computed base on the S/N analysis. Regardless of the category of the performance characteristic, a larger S/N ratio corresponds to a better performance characteristic. Therefore, the optimal level of the process parameter is the level with the highest S/N ratio. This is true for the optimization of a single performance characteristic.

In the first phase, according to Taguchi experimental design method, 16 catalyst's samples were prepared and tested. In the second phase, taking into account the results obtained from the previous phase, two samples were synthesized. While, in the third phase two samples and finally, in the last phase three more samples were prepared and tested. The particular catalyst, having the highest activity was noted and the constituents of the latter were presented. Finally, the reaction kinetic parameters have been determined for DME synthesis from syngas has been developed and correlated with experimental results.

2. Experimental

2.1. Material

The chemicals used in the present study were all analytical grades and supplied by Merck and BASF, Germany. These were copper nitrate [$Cu(NO_3)_2 \cdot 3H_2O$], zinc nitrate [$Zn(NO_3)_2 \cdot 6H_2O$], aluminum nitrate [$Al(NO_3)_3 \cdot 9H_2O$], sodium carbonate [Na_2CO_3] and ammonium carbonate [$(NH_4)_2CO_3$].

2.2. Catalyst preparation

A Solution of $Cu(NO_3)_2 \cdot 3H_2O$, $Zn(NO_3)_2 \cdot 6H_2O$, $Al(NO_3)_3 \cdot 9H_2O$ and a solution of Na_2CO_3 were co-precipitated when added simultaneously and drop wise to a beaker containing deionized water over a period of 30 min at 70 °C, under continues stirring. The precipitates formed were aged for an additional hour under continuous stirring at 70 °C. The precipitate were then filtered and washed several times with deionized water to remove residual sodium ions, and added to a suspended liquid having dehydration component (γ-alumina) and water. The final suspension was aged under stirring at 70 °C for 1 h. The precipitate was then filtered and the solid obtained was dried at 120 °C for 8 h and calcined in flowing air for 5 h. The BET surface area of the catalyst was measured using a Quantasorb apparatus (from Quantachrome Company). The XRF and XRD patterns of catalysts were also determined.

2.3. Activity measurement

Catalytic activity of all samples in converting synthesis gas to DME were studied under unsteady state conditions in a fixed bed flow reactor (i.d., 6.4 mm and length 650 mm) connected on line to a GC apparatus. The catalyst was packed in a stainless steel tube equipped with a thermocouple placed in the catalyst bed. Experiments were performed in temperatures ranging from 230 to 300 °C and a constant pressure of 8 bar g. Prior to catalytic testing the samples were crushed and sieved to fine powders. In each experimental run, about 2 g of catalyst (grain size equal to 150 μm) was loaded in the reactor having two stainless steel

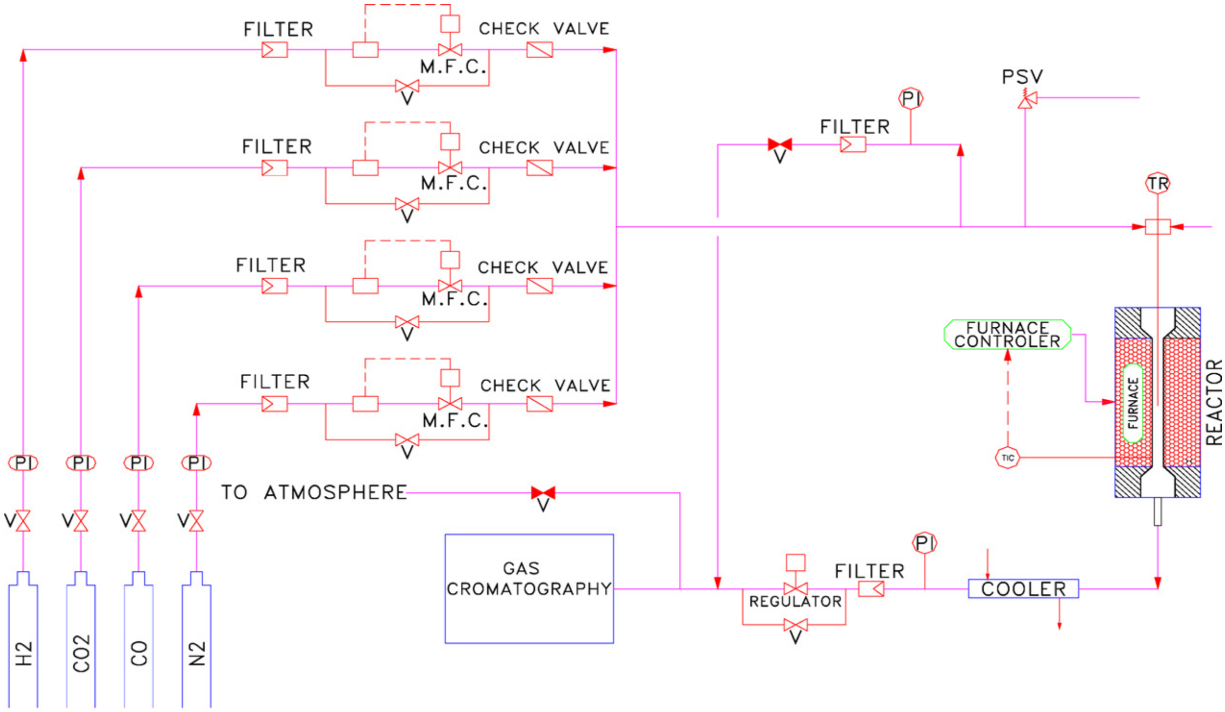

Fig. 1. Schematic diagram of the reactor setup.

supports at both ends of the catalyst bed. A schematic diagram of the experimental rig is shown in Fig. 1. The reactor system was first purged with nitrogen gas and then pressurized. The catalysts were reduced in a flowing hydrogen gas diluted with nitrogen.

A mixture of 4 vol.% CO_2, 32 vol.% CO and 64 vol.% H_2 entered the top section of the reactor that acted as a pre-heater. Three mass flow meters (Brooks, Model 5850) and a control system were used to monitor the individual gas flow rates and to provide the required gas mixtures.

A portion of the effluent gas, after reducing its pressure by a back pressure regulator, was directed to a gas chromatograph apparatus (Agilent-6890) connected on line to the system. The effluent gas was analyzed several times with 4–7 min intervals during each experimental run. The GC column was packed with Porapak Q with 80–100 mesh. The column temperature was increased steadily from 70 to 200 °C and remained at that level for 4 min. Helium was used as a carrier gas with a flow rate of 2.5 cm^3/min. The thermal conductivity detector was applied.

3. Results and discussion

3.1. Catalyst preparation

To apply the Taguchi method to the initial preparation phase, the pertinent parameters of the catalyst synthesis were selected as follows:

- (*X*) concentration of copper oxide;
- (*Y*) concentration of zinc oxide;
- (*Z*) concentration of aluminum oxide.

Four levels were considered for each parameter. An appropriate arrangement for the present system was, therefore, an L-16 configuration based on Taguchi method [6]. Arrangements of the parameters and the related levels are shown in Table 1.

In this study, an L-16 orthogonal array with 3 column and 16 rows was used. This array has 15 degree of freedom and can handle four level catalyst preparation-parameters, with 6 degree of freedom for the error. Sixteen samples (CDME-1–CDME-16) were prepared and accordingly, 16 experimental programs were performed, from which, the optimum conditions were determined. These are shown in Table 2. In the above runs, the final activity of catalysts has been taken as the response of the system. In Fig. 2 the vertical bar type presentation of the aver-

Table 1
Arrangement of parameters in L-16 presentation

Catalyst number	*X*	*Y*	*Z*
CDME-1	1	1	1
CDME-2	1	2	2
CDME-3	1	3	3
CDME-4	1	4	4
CDME-5	2	1	2
CDME-6	2	2	1
CDME-7	2	3	4
CDME-8	2	4	3
CDME-9	3	1	3
CDME-10	3	2	4
CDME-11	3	3	1
CDME-12	3	4	2
CDME-13	4	1	4
CDME-14	4	2	3
CDME-15	4	3	2
CDME-16	4	4	1

Table 2
Preparation conditions and activities of some DME synthesis catalysts

Catalysts contents	Calcination temperature (°C)	Precipitation agent	Mass ratio of γ-Al_2O_3 to total metal oxides	Copper nitrate solution (vol.%)	Zinc nitrate solution (vol.%)	Al nitrate solution (vol.%)	Slurry solution of γ-Al_2O_3 (vol.%)	Activity ((mg DME)/g cat h)[a]	DME selectivity (%)
CDME-1	350	Na_2CO_3	0.5	47.4	29.0	0	23.6	6.3	87.2
CDME-2	350	Na_2CO_3	0.5	27.8	34.3	17.0	20.9	3.4	86.8
CDME-3	350	Na_2CO_3	0.5	20.1	29.7	31.2	19.0	3.3	86.2
CDME-4	350	Na_2CO_3	0.5	15.0	29.6	37.3	18.1	2.8	85.8
CDME-5	350	Na_2CO_3	0.5	41.7	18.5	18.5	21.3	9.3	86.9
CDME-6	350	Na_2CO_3	0.5	40.6	36.2	0	23.3	4.3	87.2
CDME-7	350	Na_2CO_3	0.5	21.1	22.6	38.0	18.3	4.7	86.1
CDME-8	350	Na_2CO_3	0.5	22.6	32.3	25.4	19.7	3.2	86.5
CDME-9	350	Na_2CO_3	0.5	36.1	12.5	31.8	19.6	12.9	86.0
CDME-10	350	Na_2CO_3	0.5	26.2	18.3	36.9	18.6	6.8	86.3
CDME-11	350	Na_2CO_3	0.5	41.7	35.0	0	23.3	4.6	87.2
CDME-12	350	Na_2CO_3	0.5	31.8	35.5	11.0	21.7	3.6	87.0
CDME-13	350	Na_2CO_3	0.5	32.0	9.8	39.7	18.6	12.9	86.5
CDME-14	350	Na_2CO_3	0.5	33.4	20.6	25.9	20.1	6.9	86.3
CDME-15	350	Na_2CO_3	0.5	38.2	28.2	11.7	21.9	5.5	87.0
CDME-16	350	Na_2CO_3	0.5	38.7	38.1	0	23.2	3.9	87.2
CDME-17	350	Na_2CO_3	0.5	32.0	9.76	39.7	18.6	12.9	86.5
CDME-18	350	$(NH_4)_2CO_3$	0.5	32.0	9.8	39.7	18.6	14.3	84.9
CDME-19	350	$(NH_4)_2CO_3$	0.41	33.5	10.3	41.6	14.6	9.51	70.7
CDME-20	350	$(NH_4)_2CO_3$	0.56	30.5	9.3	37.9	22.2	11.9	84.8
CDME-21	300	$(NH_4)_2CO_3$	0.5	32.0	9.7	39.7	18.6	10.3	86.5
CDME-22	500	$(NH_4)_2CO_3$	0.5	32.0	9.7	39.7	18.6	3.8	78.9
CDME-23	700	$(NH_4)_2CO_3$	0.5	32.0	9.7	39.7	18.6	2.5	73.4

[a] Average of at least five runs with mean absolute deviation of 6–10%. The data have been obtained at 8 bar g and 250 °C.

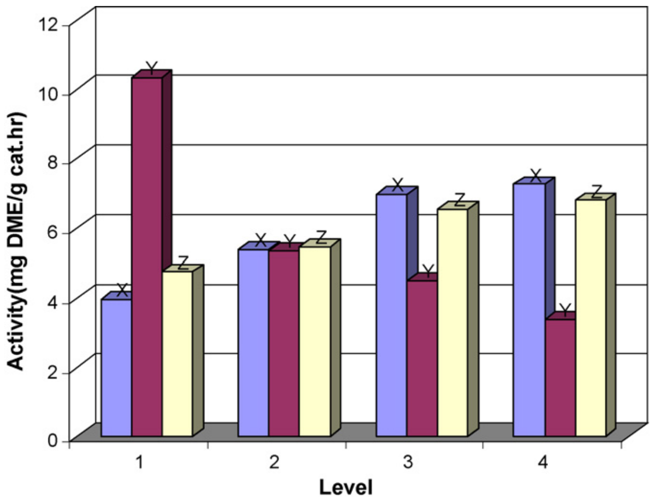

Fig. 2. Average system response to parameters at various levels.

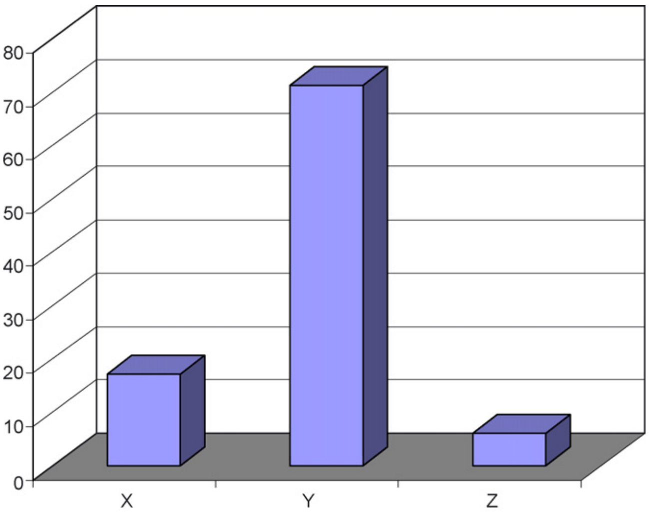

Fig. 3. Contribution of parameters to the system response.

age response of the system to various levels of parameters are demonstrated. The above results reveal the presence of certain interactions between the parameters. To determine the extent of such interactions, the response of each parameter in connection with the rest of them was considered. The results of analysis are presented in Table 3. The latter indicate some extensive interactions between *X*–*Y* and *X*–*Z* parameters. This is due to the DME synthesis from CO hydrogenation at the copper surface of catalyst [7].

Basically, a larger response corresponds to the better catalysts characteristic. However, the relative importance among the catalyst preparation parameters for the performance characteristic still needs to be known, so that the optimal combinations of the catalyst preparation parameters level can be determined more accurately. By considering the above observation the optimum conditions for the catalyst synthesis were determined as X_4, Y_1 and Z_4 (CDME-13). In other words, the optimum parameters for the present catalyst may be summarized as follows:

- concentration of copper nitrate: 31.96 vol.%;
- concentration of zinc nitrate: 9.76 vol.%;
- concentration of aluminum nitrate: 39.69 vol.%.

Analysis of the data (ANOVA table) as given in Fig. 3, indicates that the relative impact of three parameter upon the final activity of catalyst is as ZnO > CuO > Al_2O_3. In addition, the *F*-test [8] can also be used to determine which catalyst preparation parameters have a significant effect on the performance characteristic. From the Fisher tables [8] with 95% confidence, *F* 0.05, 3, 6 was found to be 4.76. The *F* values for *X*, *Y* and *Z* obtained from Taguchi method were 16.80, 66.85 and 6.52, respectively. These are greater than the corresponding values in Fisher tables. The tests are, therefore, reliable with 95% confidence. It seems that these parameters have great impact on the performance characteristic of the catalyst prepared. The calculation error was 5.426%.

Table 3
Results of percent of interaction between the catalyst preparation parameters

Preparation parameter	*X*	*Y*	*Z*
X	–	10.9	38.9
Y	10.9	–	19.3
Z	38.9	19.3	–

Referring to Fig. 2, it may be observed that excess of ZnO in catalysts has a negative effect on the activity, while presence of CuO and Al_2O_3 enhances the catalyst activity. These finding could be explained by noting that presence of copper and aluminum oxides increases the dispersion of active sites and hence promotes the surface area of catalyst, while ZnO has a reverse effect on catalyst activity. These observations may be confirmed by comparing the surface area and other data for samples CDME-1 and CDME-4, CDME-5 and CDME-8, CDME-9 and CDME-12, CDME-13 and CDME-16, as presented in Table 4.

In the second phase, the effect of precipitant nature (sodium carbonate and ammonium carbonate) on the catalysts activity was studied. Two more samples (CDME-17 and CDME-18) were prepared and tested. It was found that the activities of catalysts using ammonium carbonate as a precipitating agent were normally higher than those applying sodium carbonate. This could be due to the non-desirable effect of sodium on the catalysts activity. The Na^+ ions could reduce the number of acid sites of dehydration component (γ-alumina) of the catalyst [9] and subsequently reduce the activity of the catalyst (methanol undergoes dehydration to form DME over solid acid sites of the catalyst).

In the third phase, the influence of the acidic component (γ-alumina) of the catalysts on the activity of the latter was considered. Two more samples (CDME-19 and CDME-20) were synthesized and tested. It was observed that the highest activity was obtained at the weight ratio of 1:1 of the total metal oxide to γ-alumina (CDME-18–CDME-20). This may be due to the adequate and uniform dispersion of γ-alumina within the metal oxides phase.

Finally, in the fourth phase, the effect of calcination temperature on the catalysts activity was investigated. Accordingly,

Table 4
Certain properties and activities of some DME synthesis catalysts

Catalyst name	Calcination temperature (°C)	Total surface area (BET) (m^2/g cat)	Major crystalline phases	Activity (mg DME)/(g cat h)
CDME-1	350	143.2	CuO, ZnO, Al_2O_3	6.3
CDME-4	350	121.1	CuO, ZnO, Al_2O_3	2.8
CDME-5	350	146.8	CuO, ZnO, Al_2O_3	9.3
CDME-8	350	124.4	CuO, ZnO, Al_2O_3	3.2
CDME-9	350	240.3	CuO, ZnO, Al_2O_3	12.9
CDME-12	350	150.7	CuO, ZnO, Al_2O_3	3.6
CDME-13	350	251.3	CuO, ZnO, Al_2O_3	12.9
CDME-16	350	130.3	CuO, ZnO, Al_2O_3	3.9
CDME-18	350	257.5	CuO, ZnO, Al_2O_3	14.3
CDME-22	500	–	CuO, ZnO, Al_2O_3	3.8
CDME-23	700	65.3	CuO, ZnO, Al_2O_3	2.5

three more samples (CDME-21–CDME-23) were prepared and tested. It was found that the highest activity was obtained in case of 350 °C calcination temperature (CDME-18, CDME-21–DME-23). This may be explained by assuming that at higher calcination temperatures partial sintering of catalysts particles could be occurred and the active area of catalyst is reduced, Sohrabi and Irandokht [10] have reported a similar observation, stating that with increase in calcinations temperature the copper crystallite particle size increases and acts as backbones of water gas shift reaction.

Catalyst's activities were measured as mg of DME formed per hour per gram of catalyst. These are presented in Table 2. In Table 4, some further properties of some catalysts are given (activities were determined at 250 °C and 8 bar g).

3.2. Kinetic study

The reaction has been carried out within the temperature range of 230–300 °C, 8 bar g pressure and a wide range of catalyst to feed ratios. The results are presented in Fig. 4 and Tables 5–8.

The reaction rates given in these tables were calculated, assuming the plug flow of gas in the reactor, i.e.

$$-r_{CO} = \frac{dx_{CO}}{d(W/F_{CO_0})} \tag{1}$$

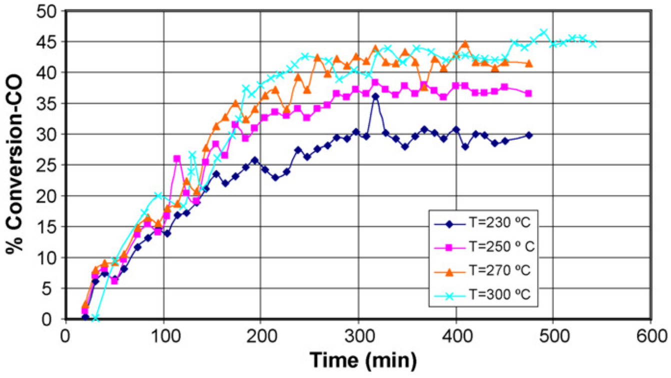

Fig. 4. Conversion of CO as a function of time at different temperatures.

$$r_{DME} = \frac{d((y_{DME.out}P)/RT)}{d(W/\phi_v)} \tag{2}$$

A number of studies on syngas transformation into liquid hydrocarbons have been made (Erena et al. [11], Peng et al. [12], Bercic and Levec [13,14] and Graff et al. [15–17]). A method similar to those proposed by Graaf and Bercic for complex reactions in isothermal fixed bed microreactors was adopted in the present study. The Graff kinetic model has been used for the transformation of syngas to methanol and that of Bercic has been applied in the synthesis of DME from methanol. These are as follows:

(a) Graff model:

$$-r_{CO} = \frac{k_1[P_{CO}P_{H_2}^{3/2} - P_{CH_3OH}/(P_{H_2}^{1/2}\mathrm{KP1})]}{(1 + k_2P_{CO} + k_3P_{CO_2})(P_{H_2}^{1/2} + k_4P_{H_2O})} \tag{3}$$

(b) Bercic model:

$$r_{DME} = \frac{-k_5(P_{CH_3OH}^2 - P_{H_2O}P_{DME}/\mathrm{KP2})}{(1 + 2(k_6P_{CH_3OH})^{1/2} + k_7P_{H_2O})^4} \tag{4}$$

The Graaf model was devised using a spinning basket reactor and applying a mixture of CO, CO_2 and hydrogen gases over commercial Cu–Zn–Al catalyst at low-pressure condition. With increasing the pressure the rate of reaction was also increased. Based on dual-site adsorption mechanism, 48 kinetics rate models were derived. Hydrogen was believed to adsorb dissociatively.

The Bercic model was developed in a differential fixed bed reactor for the conversion of methanol to dimethyl ether over γ-Al_2O_3 catalyst at low pressure. A kinetic equation based on Langmuir–Hinshelwood surface controlled reaction with dissociative adsorption of methanol was found to be correlated with the experimental results. The adsorption term for DME was neglected. In this model ($P_{CH_3OH}^2$) was a driving force term while, ($P_{H_2O}P_{DME}$/KP2) was a term describing the reversible nature of the reaction. Estimation of values for the kinetic parameters involved minimization of error. Using the nonlinear regression analysis and applying the results presented in Tables 5–8 to the relations 3 and 4, the kinetic parameters have

Table 5
Data of the reactor's outlet at 230 °C

$W_{cat.}/F_{CO}$ (g/(mol/min))	$W_{cat.}/\phi_v$ (gr/(m^3/min))	P_{H_2} (bar g)	P_{CO} (bar g)	P_{CO_2} (bar g)	P_{CH_3OH} (bar g)	P_{DME} (bar g)	P_{H_2O} (bar g)	$-r_{CO}$ (mol/(min g))	r_{DME} (mol/(min g))
260	3,731	4.96	2.47	0.32	0.003	0.13	0.12	3.3E−04	1.5E−04
896	12,658	4.6	2.29	0.48	0.03	0.3	0.3	1.2E−04	5.7E−05
1120	15,873	4.55	2.26	0.46	0.04	0.35	0.34	1.0E−04	4.5E−05
1493	21,052	4.43	2.2	0.52	0.07	0.4	0.36	7.4E−05	3.4E−05
1792	25,316	4.39	2.17	0.51	0.09	0.43	0.41	6.3E−05	2.9E−05
2240	31,746	4.34	2.15	0.49	0.13	0.45	0.44	5.3E−05	2.5E−05

Table 6
Data of the reactor's outlet at 250 °C

$W_{cat.}/F_{CO}$ (g/(mol/min))	$W_{cat.}/\phi_v$ (gr/(m^3/min))	P_{H_2} (bar g)	P_{CO} (bar g)	P_{CO_2} (bar g)	P_{CH_3OH} (bar g)	P_{DME} (bar g)	P_{H_2O} (bar g)	$-r_{CO}$ (mol/(min g))	r_{DME} (mol/(min g))
260	3,731	4.91	2.45	0.33	0.004	0.16	0.15	3.2E−4	2.2E−4
896	12,658	4.47	2.21	0.5	0.04	0.4	0.38	1.3E−4	8.8E−5
1120	15,873	4.4	2.18	0.48	0.05	0.45	0.43	1.1E−4	7.2E−5
1493	21,052	4.24	2.1	0.56	0.08	0.52	0.5	8.7E−5	5.5E−5
1792	25,316	4.18	2.06	0.55	0.11	0.56	0.54	7.6E−5	4.8E−5
2240	31,746	4.11	2.02	0.53	0.16	0.6	0.58	6.5E−5	4.1E−5

Table 7
Data of the reactor's outlet at 270 °C

$W_{cat.}/F_{CO}$ (g/(mol/min))	$W_{cat.}/\phi_v$ (gr/(m^3/min))	P_{H_2} (bar g)	P_{CO} (bar g)	P_{CO_2} (bar g)	P_{CH_3OH} (bar g)	P_{DME} (bar g)	P_{H_2O} (bar g)	$-r_{CO}$ (mol/(min g))	r_{DME} (mol/(min g))
260	3,731	5	2.39	0.4	0.003	0.14	0.07	4.7E−04	2.1E−04
896	12,658	4.71	2.07	0.67	0.03	0.36	0.17	1.8E−04	8.3E−05
1120	15,873	4.69	2	0.69	0.04	0.4	0.17	1.4E−04	6.8E−05
1493	21,052	4.58	1.89	0.79	0.07	0.46	0.2	1.1E−04	5.1E−05
1792	25,316	4.55	1.85	0.8	0.1	0.5	0.21	9.2E−05	4.4E−05
2240	31,746	4.52	1.78	0.82	0.14	0.53	0.21	7.5E−05	3.8E−05

Table 8
Data of the reactor's outlet at 300 °C

$W_{cat.}/F_{CO}$ (g/(mol/min))	$W_{cat.}/\phi_v$ (gr/(m^3/min))	P_{H_2} (bar g)	P_{CO} (bar g)	P_{CO_2} (bar g)	P_{CH_3OH} (bar g)	P_{DME} (bar g)	P_{H_2O} (bar g)	$-r_{CO}$ (mol/(min g))	r_{DME} (mol/(min g))
260	3,731	5.06	2.35	0.44	0.003	0.13	0.01	3.7E−04	1.7E−04
896	12,658	4.86	1.97	0.78	0.03	0.33	0.3	1.3E−04	7.0E−05
1120	15,873	4.87	1.89	0.82	0.04	0.37	0.01	1.0E−04	5.9E−05
1493	21,052	4.8	1.76	0.94	0.07	0.43	0.003	7.6E−05	4.6E−05
1792	25,316	4.78	1.71	0.96	0.09	0.46	0.003	6.6E−05	4.0E−05
2240	31,746	4.74	1.63	0.98	0.13	0.5	0.01	5.4E−05	3.3E−05

Table 9
Kinetic parameters

Kinetic constant	Temperature (°)				K_{0I}	E/R
	230	250	270	300		
K_1 (mol min^{-1} bar^{-2} g^{-1})	8.7E−6	4.2E−05	2.6E−05	1.2E−05	1.1E−11	−7963
K_2 (bar^{-1})	0.235	0.324	0.445	0.547	2.9E+02	3561.6
K_3 (bar^{-1})	5.568	3.324	1.164	0.948	9.6E−07	−7812.4
K_4 (bar$^{-1/2}$)	4.96	3.392	0.258	0.01	8.2E−23	−26755
KP1(bar^{-2})	0.027	0.021	0.012	0.007	2.5E−07	−5855.5
K_5 (mol min^{-1} bar^{-2} g^{-1})	0.008	0.006	0.004	0.001	6.1E−10	−8322.8
K_6 (bar^{-1})	7.786	11.055	31.29	46.712	5.4E+07	7940.1
K_7 (bar^{-1})	8.39	6.81	6.19	5.14	1.7E−01	−1957.2
KP2	0.023	0.017	0.008	0.007	1.3E−06	−4880.6

Table 10
Comparison between calculated and literature data

	E_1 (kJ/mol)	H_2 (kJ/mol)	H_3 (kJ/mol)	H_4 (kJ/mol)	E_5 (kJ/mol)	H_6 (kJ/mol)	H_7 (kJ/mol)
Calculated value	66.2	29.6	64.9	222.4	69.2	66	16.3
Literature value	51.8	58.1	67.4	104.5	143.7	70.5	41.1

been calculated. The data are given in Table 9. The calculated values of activation energies are compared with the data available in the literature (Table 10).

4. Conclusion

In the present study, the activities of DME synthesis catalysts were gradually improved during a four-phase preparation program and the following observations were made:

(a) By applying the Taguchi method and analysis of data, certain interactions between the preparation parameters were noted. The appropriate experimental conditions, predicted from Taguchi method were (X_4, Y_1 and Z_4).
(b) ZnO was found to have the greatest impact on the catalysts activity.
(c) The catalysts prepared using ammonium carbonate as the precipitant were more active in comparison with those applying sodium carbonate.
(d) The highest activity was obtained with a catalyst containing 50 wt.% of γ-alumina and calcinated at 350 °C.
(e) A kinetic expression for syngas transformation to DME based on Graaf methanol synthesis and Bercic dehydration models has been derived and correlated with the experimental results over a range of temperatures. The degree of agreement between the two sets of data was 90–95%.

References

[1] J. BØgild Hansen, B. Voss, F. Joensen, I. Dcra-Siguroavdottir, Large scale manufacture of dimethyl ether a new alternative diesel fuel from natural gas, in: SAE Technical Paper Series, International Congress & Exposition, Detroit, Michigan, February 27–March 2, 1995.
[2] G. Sam Samdani, Chementator, Chem. Eng. (1995) 17–18.
[3] T. Fleisch, C. McCarthy, A. Basu, C. Udovich, Demonstration of ULEV emissions on a navistar diesel engine fueled with dimethyl ether, in: SAE Technical Paper Series, International Congress & Exposition, Detroit, Michigan, February 27–March 2, 1995.
[4] Z. Nle, H. Liu, D. Liu, W. Ying, D. Fang, Intrinsic kinetics of dimethyl ether synthesis from syngas, J. Nat. Gas Chem. 14 (2005) 22–28.
[5] Q. Ge, Y. Huang, F. Qiu, S. Li, Bifunctional catalysts for conversion of synthesis gas to DME, Appl. Catal. 167 (1998) 23–30.
[6] G. Taguchi, S. Konishi, Orthogonal Arrays and Linear Graphs, American Supplier Institute Press, Dearborn, MI, 1987.
[7] G. Qi, X. Zheng, J. Fei, Z. Hou, A novel catalyst for DME synthesis from CO hydrogenation, J. Mol. Catal. 176 (2001) 195–203.
[8] R.A. Fisher, Statistical Methods for Research Workers, Oliver & Boyd, London, 1952.
[9] M. Xu, J.H. Lunsford, D.W. Goodman, A. Bhattacharyya, Synthesis of DME from methanol over solid acid catalysts, Appl. Catal. 149 (1997) 289–301.
[10] M. Sohrabi, A. Irandokht, Synthesis and activity measurement of some water gas shift reaction catalysts, React. Kinet. Catal. Lett. 80 (2) (2003) 303–309.
[11] J. Erena, J.M. Arandes, J. Bilbao, A.G. Gayubo, H.I. De lasa, Conversion of syngas to liquid hhydrocarbons over a two-component (Cr_2O_3-zno and zsm-5 zeolite) catalyst: kinetic modeling and catalyst deactivation, Chem. Eng. Sci. 55 (2000) 1845–1855.
[12] X.D. Peng, B.A. Toseland, P.J.A. Tijm, Kinetic understanding of chemical synergy under LPDME conditions—once through applications, Chem. Eng. Sci. 54 (1999) 2787–2792.
[13] G. Bercic, J. Levec, Intrinsic and global reaction rate of methanol dehydration over γ-Al_2O_3 pellets, Ind. Eng. Chem. Res. 31 (1992) 1035–1040.
[14] G. Bercic, J. Levec, Catalytic dehydration of methanol to DME. Kinetic investigation and reactor simulation, Ind. Eng Chem. Res. 32 (1993) 2478–2484.
[15] G.H. Graaf, J.G.M. Winkelman, E.J. Stamhuis, A.A.C.M. Beenakers, Kinetics of three phase methanol synthesis, Chem. Eng. Sci. 43 (8) (1988) 2161–2168.
[16] G.H. Graaf, P.J.J.M. Sijtsema, E.J. Stamhuis, G.E.H. Joosten, Chemical equilibria in methanol synthesis, Chem. Eng. Sci. 41 (11) (1986) 2883–2890.
[17] G.H. Graaf, E.J. Stamhuis, A.A.C.M. Beenakers, Kinetics of low-pressure methanol synthesis, Chem. Eng. Sci. 43 (12) (1988) 3185–3195.